The geochemistry of mafic and ultramafic rocks from the Archaean greenstone belts of Sierra Leone

H. R. ROLLINSON

Department of Geography and Geology, The College of St Paul and St Mary, The Park, Cheltenham, Glos. GL50 2RH, UK

ABSTRACT. The Archaean (c. 2800 Ma) ultramafic rocks in eastern Sierra Leone cut basalt lavas and are mostly olivine-rich cumulates either iron-rich (Fo_{85-86}) and derived from a basaltic or picritic parent, or more magnesian (Fo_{92-93}) derived from an ultramafic melt with c. 18-25 wt. % MgO. In central Sierra Leone the ultramafic rocks are lavas predating tholeiitic basalts.

The basalts show a wide variation in Zr/Y, suggesting that garnet was present in the source region of some of these rocks but not others. This implies that melting took place at different depths in the mantle. The REE evidence for basaltic rocks in the upper part of the Nimini belt succession suggests that they were derived from a mantle source region which had already suffered melt extraction. Ti/Zr ratios in the basaltic rocks are also variable and individual belts define different trends on a Ti vs. Zr plot implying that the basaltic rocks evolved in geographically distinct magma chambers. It is likely that the basaltic rocks evolved from a parental liquid with Ti/Zr = 90 via shallow level crystal fractionation. The source region for these rocks therefore had a lower than chondritic Ti/Zr.

There are two possible models for the basaltic and ultramafic magmas in the Sierra Leone greenstone belts. First that the ultramafic and basaltic liquids were derived from mantle diapirs of differing size, but originating in the same region of the mantle. Ultramafic liquids were produced in small diapirs, which store large melt fractions, and basaltic liquids in larger diapirs which segregate larger melt fractions. A second model is based upon the double diffusion process suggested for magma chambers at mid-ocean ridges and involves a transient magma chamber from which basalts, derived from parental ultramafic liquids, are erupted, with ultramafic liquids rising directly to the surface when the magma chamber is frozen. The available data does not discriminate between these two models.

THE Archaean greenstone belts of Sierra Leone form a series of tightly folded, subparallel belts, up to 130 km long, metamorphosed to amphibolite and granulite facies. They contain thick sequences of mafic and ultramafic rocks overlain by grey-wacke turbidites and quartzites and evolved on or adjacent to ancient continental crust (Williams, 1978; Rollinson, 1978). There are rapid sedimentary facies variations along the length of individual belts and geochemical evidence presented below suggests that the belts represent separate volcanic centres which evolved independently of each other. New Rb-Sr and Pb-Pb age determinations (Beckinsale et al., 1980; Rollinson and Cliff, 1982) on the underlying gneisses and on later cross-cutting granites constrain the age of the greenstone belts to the time interval 2770-2970 Ma.

Previous geochemical work in the northern part of the Kambui belt (Andrews-Jones, 1968) showed that the greenstones were composed of a series of tholeiitic basalts intruded by ultramafic sills. In this study tholeiitic amphibolites and ultramafic rocks were collected from the Sula Mountains, the Nimini and Kambui Hills, the Gori Hills, and the Mano Moa granulite greenstone belts (fig. 1) in order to (a) compare the chemistry of the basaltic rocks from the different belts, (b) to determine the relationship between the basaltic and ultramafic rocks, and (c) to set limits on their origin. The emphasis in this paper is on petrological processes in order that these may be used to constrain models for the genesis of the Sierra Leone greenstone belts.

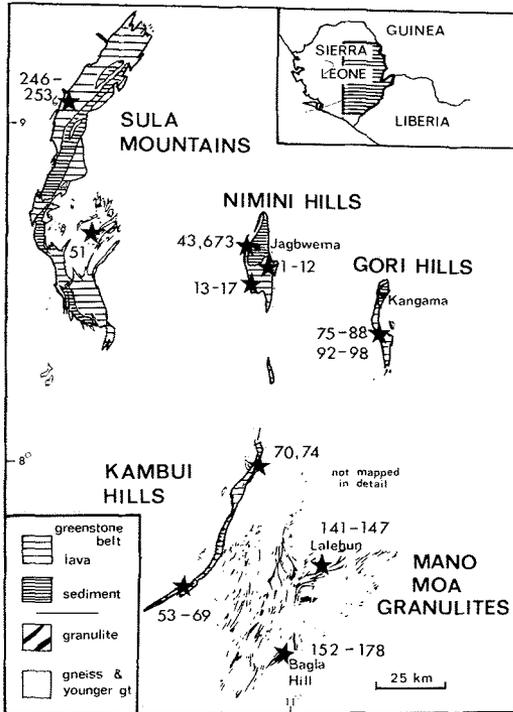Reviews of the Archaean geology of Sierra Leone

FIG. 1. Geological map of eastern Sierra Leone showing the distribution of the greenstone belts and sample localities (stars). Granulites are restricted to the southeastern corner of the map. (In the key gt = granite.)

and the stratigraphy of the West African greenstone belts are given by Williams (1978) and Rollinson (1978) respectively. However, much of the field work reported in this paper in the Nimini, Gori, and Kambui Hills greenstone belts was carried out by the author whilst employed by the Geological Survey of Sierra Leone and is contained in unpublished reports to the Geological Survey of Sierra Leone (1973–5).

Stratigraphy

Of the five greenstone belts considered in this paper the stratigraphy of the Nimini Hills belt is the best established and is summarized in fig. 2. The succession is subdivided into two formations, a lower, meta-igneous formation, dominated by amphibolites and an upper sedimentary formation dominated by greywacke turbidites. The lowest exposed part of the meta-igneous succession comprises interbanded tremolite schist, serpentinite, and amphibolite with minor quartzite and pelitic schist. This is overlain by a sequence of massive and pillowed amphibolites 2.5 km thick. The sedi-

mentary formation overlies the meta-igneous formation conformably and comprises a monotonous sequence of greywacke turbidites 2 km thick, with minor horizons of hornblendic quartzite. Banded ironstone 30 m thick is present at the base of the sedimentary formation close to the junction with the underlying amphibolites; cross bedded quartzites are present at the top of the sedimentary formation. In the western part of the belt there is a 1 km thick, discordant, layered tremolite schist–serpentinite body in the meta-igneous formation which is interpreted as an intrusive ultramafic complex.

A similar stratigraphical succession to that described from the Nimini Hills has been described from the Sula Mountains greenstone belt by MacFarlane et al. (1981) who recognized a lower amphibolite and ultramafic schist formation (the Sonfon Formation) and an upper sedimentary formation (the Tonkolili Formation) composed of clastic sediments and thin layers of siliceous volcanics.

One of the main features of the Sierra Leone greenstone belts is that they show marked variations in stratigraphy both within and between belts. Stratigraphic variation within belts is well illustrated in the Nimini Hills and Kambui Hills belts (fig. 2) which were formerly a single continuous belt (fig. 1). Stratigraphic variation between greenstone belts in the West African Archaean was described by Rollinson (1978). There is a gradation in size of belt, stratigraphic thickness and metamorphic grade from the Sula Mountains to the Mano Moa Granulites (fig. 1). The Sula Mountains belt is 130 km long, has a succession 6.5 km thick, and is metamorphosed to amphibolite facies; in contrast the Mano Moa granulites represent a highly disrupted, thin (c. 1 km) greenstone belt sequence, occurring as lenses up to 20 km long, enclosed in tonalitic gneiss and metamorphosed to granulite facies.

The contacts between the greenstone belts and enclosing granitic gneisses are obscured by migmatization and the intrusion of young potassic granites. However, the presence of large granite clasts in conglomerates in the upper part of the succession in the Gori Hills and the Sula Mountains belts (Marmo, 1962; Wilson and Marmo, 1958) suggest the proximity of sialic crust during at least the later stages of development of the greenstone belts. Furthermore, MacFarlane et al. (1981) showed from structural mapping the existence of gneisses which predate the formation of the greenstone belts, although radiometric age determinations on these gneisses are at present equivocal (Beckinsale et al., 1980; Rollinson and Cliff, 1982). It should be noted that in the absence of an observed

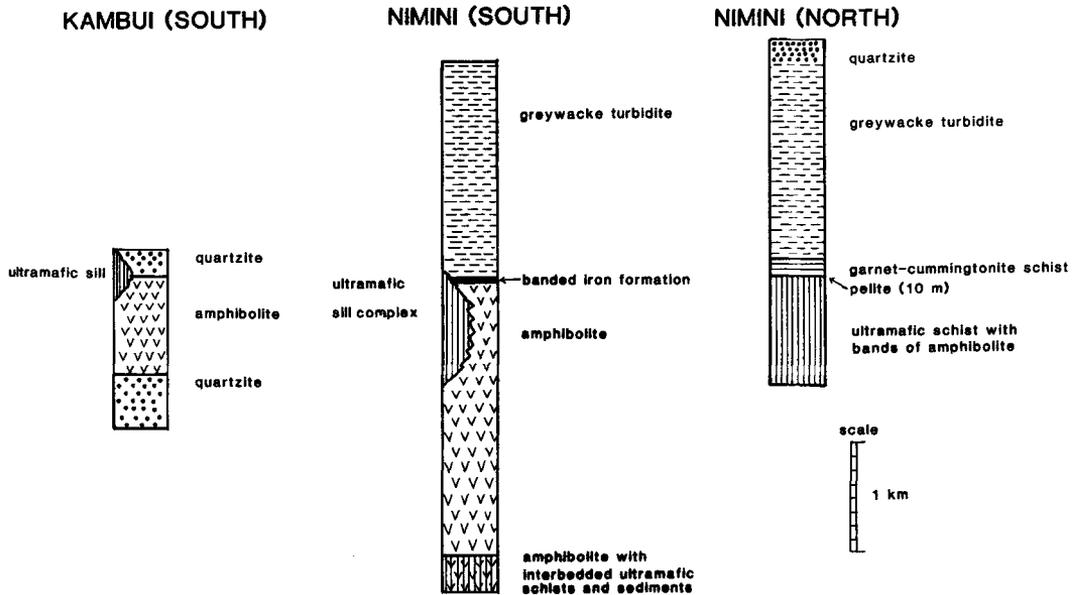**KAMBUI (SOUTH)**   **NIMINI (SOUTH)**   **NIMINI (NORTH)**

FIG. 2. Stratigraphical sections through the Nimini-Kambui belt. Note that the distance between the Kambui (south) and the Nimini (south) sections is 120 km and between the Nimini (south) and Nimini (north) sections is 25 km.

base to the succession in the Sierra Leone greenstone belts it is possible that the stratigraphy described above represents only part of a thicker greenstone sequence.

Major lithologies

Ultramafic Rocks. In the Sula Mountains there is a thick succession (4 km) of fine-grained tremolite–chlorite schists, which at one locality show pillows. They are interbedded with, and overlain by, pillowed amphibolites and are thought to represent metamorphosed ultramafic lavas. In the smaller greenstone belts of eastern Sierra Leone (i.e. the Nimini, Gori, and Kambui belts) the ultramafic rocks are coarse- to fine-grained tremolite–chlorite schists and serpentinites. There is no evidence of pillows or spinifex textures and relict igneous layering is common, indicated by horizons rich in serpentinized olivine in tremolite–chlorite schist. There are also ultramafic units rich in clinopyroxene. Near the base of the succession in the Nimini belt there is a layered ultramafic unit, conformably interbedded with amphibolite and chert, which contains abundant clinopyroxene in a fine-grained matrix, now recrystallized to tremolite, and which probably represents an ultramafic flow. At Hanga in the Kambui belt, dunite shows well-developed olivine-rich and chromite-rich gravity stratified units (Dunham *et al.*, 1958), from which facing directions can be established. Most of the ultra-

mafic rocks in the greenstone belts of eastern Sierra Leone are discordant with respect to the enclosing amphibolites and metasediments indicating that they are intrusive and post-date the amphibolites; the intrusions vary in thickness from 80 to 1000 m.

Amphibolites. Amphibolites are both massive and pillowed. Some pillow lavas have vesicular tops in which the vesicles are infilled with calcite and quartz. Facing directions can be obtained from the pillow lavas. Massive amphibolites sometimes have chilled margins and may in part represent sills and dykes.

Sediments. The dominant sedimentary rocks are quartzite, greywacke, and banded ironstone. They are normally prominent in the upper part of the succession but in the southern part of the Kambui belt quartzites are the lowest unit present (fig. 2). Well-preserved sedimentary structures are often present and facing directions were determined from cross bedding and scours in the quartzites and from graded bedding and ripple marks in the greywacke turbidites. There are conglomeratic horizons in the upper part of the succession in most of the belts, generally of an intraformational nature, carrying clasts of quartzite, amphibolite, and mica schist but more rarely granite clasts are also present. Fuchsite-bearing quartzites are present in most of the belts and in the Gori Hills there is a thin horizon of a high-alumina fuchsite rock (andalusite–fuchsite–corundum–quartz–rutile) of the type recently described by Schreyer *et al.* (1981).

There are marked sedimentary facies variations in some of the belts; these are particularly marked in the northern part of the Gori Hills where pelitic schists in the west pass into quartzites in the east over a distance of 3 km.

Petrography

All the rocks analysed in this study have been metamorphosed to amphibolite or granulite facies. Sample collected from the Sula Mountains, Nimini, Gori, and Kambui Hills show amphibolite-facies mineral assemblages and samples from the Mano Moa granulites, granulite-facies assemblages.

Basaltic compositions. Most rocks of basaltic composition were totally recrystallized during metamorphism and only a few samples, from the centre of the Nimini and Sula Mountains belts show relict igneous textures. These rocks outcrop in areas where pillow lavas are best preserved. They show a relict ophitic texture with plagioclase laths in a relatively fine-grained hornblende-rich matrix. With increasing recrystallization the plagioclase laths are pseudomorphed by fine-grained plagioclase and intergrown with hornblende porphyroblasts and sphene. Some amphibolites also show aggregates of granular plagioclase, pseudomorphing plagioclase phenocrysts, in a fine-grained matrix of hornblende. There are radiating sprays of hornblende in the groundmass which may be pseudomorphs after clinopyroxene variolites. Plagioclase phenocrysts are also present in amphibolites in the Kambui belt, where they are partially replaced by epidote, calcite, biotite, and hornblende. Some amphibolites show rotated and partially recrystallized hornblende megacrysts up to 5 mm long in a matrix of fine-grained hornblende, which may be pseudomorphs after clinopyroxene phenocrysts. In the Nimini belt there are pseudomorphs with cores of poikiloblastic hornblende and rims of plagioclase set in a matrix of fine-grained hornblende and plagioclase which are reminiscent of skeletal clinopyroxenes in quenched basaltic liquids.

Amphibolites from the lowest part of the Nimini succession, outcropping at the margin of the belt and in the Gori and Kambui belts have a metamorphic texture. They are medium grained with a granular texture and appear both massive and banded. Epidote and sphene are common accessory minerals and there are thin irregular veins rich in plagioclase, quartz, epidote, sphene, and sulphides.

In the Mano Moa granulites basaltic rock compositions contain the mineral assemblage: orthopyroxene-clinopyroxene-plagioclase-hornblende (olive-green)-ilmenite-magnetite $\pm$ biotite. Most rocks have a granular texture; hornblende, which forms between 15 and 35% of the rock, occurs as equant grains in textural equilibrium with pyroxene, and biotite generally forms less than 2% of the rock. The only indication of relict textures are fine- and medium-grained granulites, which may reflect original variations in grain size, and a single pseudomorph of granular plagioclase after a plagioclase phenocryst in a fine-grained granulite.

Ultramafic rocks. Under amphibolite-facies conditions

ultramafic rocks recrystallized to tremolite-chlorite schists and serpentinites; relict grains of olivine, clinopyroxene, and spinel are preserved in some samples. Serpentinites contain elliptical grains of olivine, up to 4 mm across showing varying stages of replacement by serpentine, tremolite, and chlorite, and with textures typical of igneous cumulates. Olivine is overgrown by tremolite, both minerals are replaced by serpentine and subsequently partially replaced by chlorite. There is no evidence of new olivine growth during metamorphism and from the textural evidence presented above it is clear that olivine is the earliest mineral present and may therefore be a relict igneous phase.

Tremolite-chlorite schists from the Gori Hills contain abundant rotated tremolite porphyroblasts which have cores of uralite containing small rounded grains of magnetite; these porphyroblasts are pseudomorphs after either ortho- or clinopyroxene. Fine-grained tremolite schist from an ultramafic flow near the base of the succession in the Nimini belt contains relict grains of chrome magnetite, olivine, and clinopyroxene, in a fine-grained matrix of tremolite. Clinopyroxene forms abundant, equant grains with corroded margins; olivine is serpentinized and forms elliptical grains and chrome magnetite is very fine grained (less than 0.1 mm) and defines a fine banding, which is overgrown by the olivine, clinopyroxene, and tremolite.

Both the tremolite schists and the serpentinites are cut by irregular veins rich in talc and carbonates.

Chromitites and dunites with chromite from Hanga, in the Kambui belt contain polygonal grains of chromite and olivine up to 5 mm across, and small, uralitized grains of orthopyroxene. Olivine is serpentinized and rimmed with chlorite in the dunites, but is totally replaced by chlorite in the chromitites; chromite grains are corroded at their margins and partially replaced by chlorite. Chlorite grains also cut through the chromitites and dunites.

Granulite facies ultramafic rocks contain the mineral assemblages orthopyroxene-olivine-hornblende (24–45%), orthopyroxene-hornblende (40–50%)-opaques-spinel, orthopyroxene-clinopyroxene (10%)-hornblende (35%)-olivine. There is a small amount of late biotite in most samples but in sample 162 it forms up to 50% of the rock and contains abundant inclusions of zircon. Ultramafic granulites have an equigranular texture and olivine, when present, forms small, rounded grains varying in diameter from 1 to 4 mm, and is often partially serpentinized. There is no indication of original textures in the ultramafic granulites.

Mineral chemistry

Electron probe traverses across plagioclase phenocrysts from amphibolite 74 show zoning from An_{63} (core) to An_{29} (rim); groundmass plagioclase, on the other hand, is unzoned and is An_{47}. The phenocrysts are in part replaced by epidote, calcite, biotite, and hornblende and have changed composition during metamorphism, although the core compositions are typical of unaltered igneous phenocrysts in basalts.

Olivines from amphibolite facies ultrabasic rocks vary from Fo_{95} to $Fo_{84.5}$ (Table I) and individual grains show slight zoning. Some of the range in composition is due to metamorphic re-equilibration. In dunite from Hanga in the Kambui belt, olivine (Fo_{95}) is unzoned and coexists with slightly zoned chromite; olivine–chromite pairs yield temperatures in the range 540 °C (rim) to 600 °C (core) on the olivine–spinel thermometer of Roedder *et al.* (1979). These temperatures are consistent with estimates of metamorphic temperatures in the Nimini and Gori Hills belts (Rollinson, 1982) and imply the redistribution of Fe and Mg between olivine and chromite during the metamorphism, so that the olivine is now more magnesian than in the original igneous rock. Minor element compositions in olivines in amphibolite-facies rocks fall into the field of terrestrial igneous rocks (Simkin and Smith, 1970) for Ni but show some scatter for Mn, suggesting some metamorphic re-equilibration.

In granulite-facies ultramafic rocks olivine is unzoned and varies from Fo_{77} to $Fo_{82.5}$ (Table I). A comparison of olivine compositions from granulite-facies and amphibolite-facies ultrabasic rocks with the same bulk MgO/(MgO + FeO) ratio shows that the olivines are more magnesian in amphibolite-facies rocks and implies some change in mineral Mg/Fe ratios during metamorphism. There is no textural evidence to suggest that the Fe-rich olivine in granulite-facies rocks is original. However, the origin of the olivine in the amphibolite-facies ultramafic rocks is more equivocal. Textural evidence suggests that it is igneous but the

mineral chemistry suggests that there has been re-equilibration during metamorphism and that igneous compositions are not preserved.

Spinel compositions vary from chromite to magnetite (Table I). At Hanga chromite from dunite is slightly zoned with core to rim values for Cr/(Cr + Al) and $Fe_{tot}/(Fe_{tot} + Mg)$ from 0.61 to 0.63 and 0.56 to 0.60 respectively. This is due at least in part to re-equilibration with olivine during the metamorphism. In sample 673 from an ultramafic flow in the Nimini belt, rounded magnetite grains in olivine and clinopyroxene contain 1.9 % Cr_2O_3 and 0.48 % NiO (Table I). Relict grains of clinopyroxene in the same sample have very high Ca contents with Ca/(Ca + Mg + Fe) = 0.5; Mg/(Mg + Fe) is also high (0.94) and Al_2O_3 is low (0.2 to 0.9 wt. %).

Metamorphism

P-T conditions for the peak of metamorphism in the Sierra Leone greenstone belts and granulites have been calculated for pelitic assemblages as follows: Nimini Hills greenstone belt 565 $\pm$ 50 °C, 5.5 $\pm$ 0.5 kbar; Gori Hills greenstone belt 565 $\pm$ 50 °C, 4.9 $\pm$ 2.5 kbar; Mano Moa granulites 770 $\pm$ 50 °C, 7.5 $\pm$ 1.5 kbar (Rollinson, 1982). In view of the extensive metamorphic recrystallization at amphibolite and granulite facies of the samples used in this study, attention is paid in this section to the way in which the geochemistry may have been controlled by the metamorphism.

Field and petrographic evidence for the mobility of major elements on the scale of a few millimetres

Table I   Electron microprobe analyses of Minerals

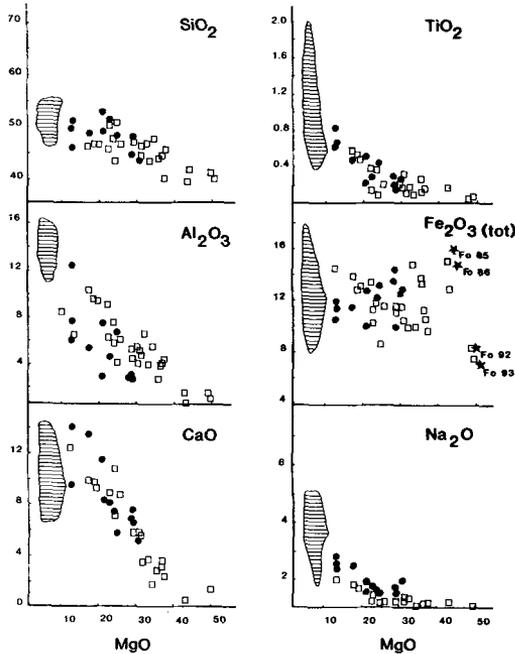|	Granulite facies			Amphibolite facies					Spinel	Spinel	Clino-pyroxene
Rock	Olivine 108	Olivine 170B	Olivine 160	Olivine 51	Olivine 58	Olivine 70	Olivine 673		673	70	673
SiO_2	39.08	39.30	38.71	39.36	39.63	41.86	40.54	SiO_2	.00	.00	53.59
FeO_{tot}	20.19	16.62	20.72	14.77	13.88	4.83	9.42	TiO_2	.07	.14	.10
MnO	.31	.23	.30	.29	.49	.07	.74	Al_2O_3	.00	19.78	.58
MgO	40.14	43.86	39.35	45.19	45.58	53.53	49.23	FeO_{tot}	87.50	17.89	1.94
CaO	.04	.01	.00	.02	.01	.00	.02	MnO	.14	.43	.17
NiO	.51	.32	.31	.33	.36	.49	.30	MgO	.64	13.21	17.36
Cr_2O_3	nd*	.00	nd	.00	.01	.02	.03	CaO	.06	.01	25.48
								NiO	.48	nd	.05
								Cr_2O_3	1.90	48.13	.06
TOT	100.27	100.43	99.39	99.96	99.96	100.81	100.28	TOT	90.79	99.60	99.33
Fo_{mean}	78	82.5	77	84.5	85.4	95	90				
$Fo_{at core}$	78	82.5	77	84.5	85	95	89.5				
								$mg/mg+fe_{(tot)}$	.013	0.568	0.941
No. of anals.	4	5	4	3	5	5	4		5	3	4

*nd: not determined

FIG. 3. Plot of major elements *vs.* MgO for 104 basaltic and ultramafic rocks from the Sierra Leone greenstone belts. Symbols: horizontal shading—basalts; filled circles—granulite-facies ultramafic rocks; open squares—amphibolite-facies ultramafic rocks; stars—olivine compositions.

during and after metamorphism comes from the metamorphic mineralogy of the analysed samples and the presence of occasional, thin (1–2 mm) veins cutting the metamorphic fabric. In the amphibolites the veins contain one or more of the following minerals; quartz, plagioclase, epidote, carbonate, sulphides, and more rarely sphene. In the ultramafic rocks there are veins of talc and carbonates and more rarely serpentine and magnetite.

Studies by Elliott (1973) and Muecke *et al.* (1979) show that TiO_2 is relatively immobile during medium- to high-grade metamorphism in basic igneous rocks and so major elements are plotted against TiO_2 for the Nimini basalts as a test of metamorphic alteration (fig. 5). Samples from the centre of the belt, where there are pillows and relict igneous textures preserved and where discordant mineral veins are rare, show good trends for $Fe_2O_{3(tot)}$ and P_2O_5, poor trends for MgO, Al_2O_3, and K_2O and a scatter for SiO_2, CaO, and Na_2O (fig. 5). Samples from the lowest part of the succession, collected at the margin of the belt, where metamorphic recrystallization is total, show much higher concentrations of K_2O and do not conform to any of the trends described above

except for Fe_2O_3 and to a lesser extent Al_2O_3. These data suggest that on the scale of sampling (i.e. 10's of cm) Fe_{tot} was the least mobile element and that Mg, Al, and P were relatively immobile during amphibolite-facies metamorphism of the Nimini belt basalts.

Rocks with more than 10% MgO have high water contents (up to 13%) and plots of major elements against Al_2O_3 and TiO_2 show a scatter against all oxides except P_2O_5, MgO, and to a lesser extent $Fe_2O_{3(tot)}$ (not shown), suggesting that there has been significant redistribution of the major elements during the metamorphism of the ultramafic rocks. However, variation diagrams plotted against MgO, one of the less mobile elements during metamorphism, do show poorly constrained, but regular trends for the oxides SiO_2, CaO and the trace elements Ni and Cr as well as TiO_2 and Al_2O_3 (figs. 3 and 4), which are throught to reflect chemical variations in the original igneous suite. On the Al_2O_3–MgO diagram (fig. 3) there is a
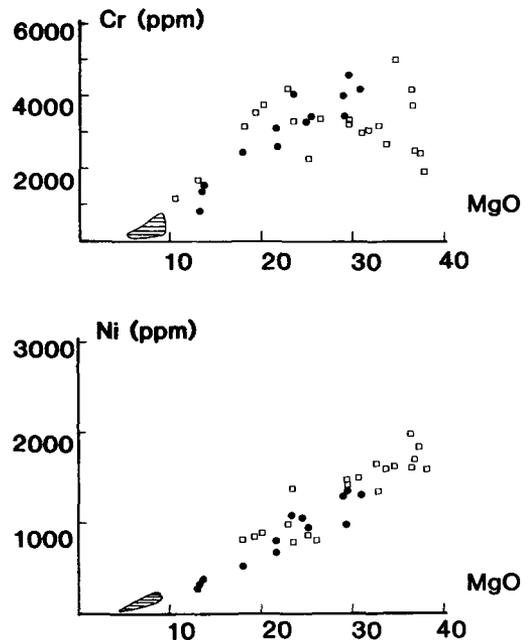

FIG. 4. Plot of Ni and Cr *vs.* MgO for basaltic and ultramafic rocks from the Sierra Leone greenstone belts. Symbols as in fig. 3.

scatter about a poorly defined trend, which can in part be explained by the fact that ultramafic rocks from the Mano Moa granulites have consistently lower Al_2O_3 values for a given MgO content than rocks from the greenstone belts. This may represent the systematic loss of either MgO or Al_2O_3 from
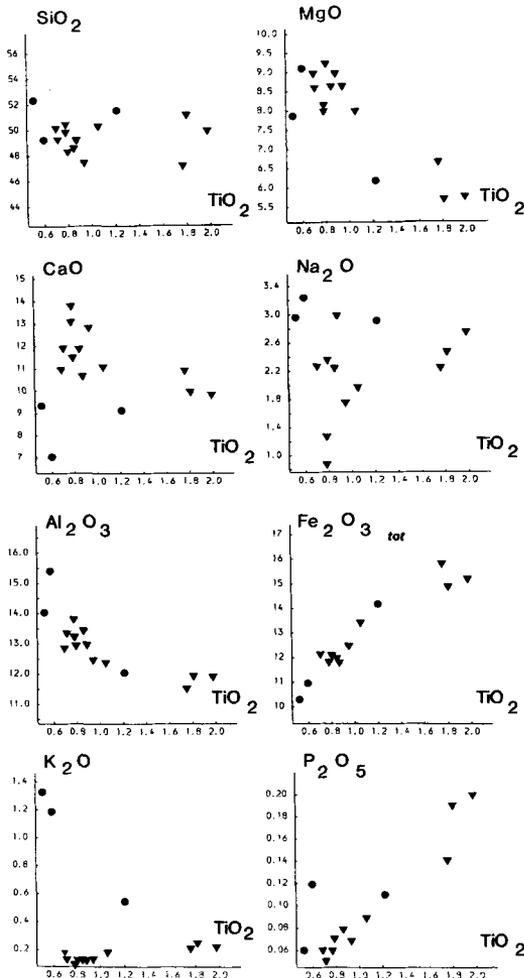
FIG. 5. Plot of major elements vs. TiO_2 for basaltic rocks from the Nimini Hills belt. Symbols: circles—lower section (margin of belt); triangles—upper section (centre of belt).

Major element variations in the ultramafic rocks are therefore a function of fractionation in magmas with different starting compositions and their subsequent alteration during metamorphism.

Geochemistry

Ultramafic rocks. Field, petrographic, and textural evidence presented above for the ultramafic rocks show that the majority of the high-MgO rocks are derived from cumulates. Incompatible element concentrations further support this view. In amphibolite facies ultramafic rocks Zr is in the range 0–14 ppm and is generally less than 10 ppm; Y is in the range 3–11 ppm and is generally less than 6 ppm. These values are close to and in some cases less than suggested mantle values for the Archaean (Nesbitt and Sun, 1976; Sun and Nesbitt, 1977) and are consistent with the accumulation of a phase or phases low in incompatible elements. Petrographic evidence suggests that olivine is the main fractionating phase. However, some samples from a layered sill or flow in the Gori Hills belt contain pseudomorphs after an unidentified pyroxene and show a systematic increase in MgO with decreasing CaO, indicating that the main fractionating phase was either olivine or orthopyroxene. Calculated partition coefficients for the fractionating phase, using the inversion method of Allegre et al. (1977) with Zr as the abscissa, are Cr 1.5, Ni, 1.6, Ti 0.042, and Y 0.2; these are closer to published partition coefficients for orthopyroxene than for olivine or for clinopyroxene (Pearce and Norry, 1979; Hart and Davis, 1978; Pearce, 1978) and suggest that in this case orthopyroxene was the main fractionating phase.

Since there is no direct evidence for the chemical composition of the liquids parental to the ultramafic rocks an attempt is made to calculate this from the compositional relationship known to exist between olivine and mafic and ultramafic liquids (Roedder and Emslie, 1970). On the $Fe_2O_{3(tot)}$ vs. MgO diagram (fig. 3) ultramafic rocks show a scatter of Fe_2O_3 values between basaltic compositions and MgO = 50%. However, at high MgO concentrations the bulk compositions of some serpentinites plot very close to the olivine compositions Fo_{92-93} and Fo_{85-86}. Petrographically the iron-rich samples, with a bulk composition close to Fo_{86} are serpentinized olivine cumulates, now totally replaced by serpentine, magnetite, chlorite, and a small amount of calcite. The iron-poor samples, with a bulk composition approaching Fo_{93} are partially serpentinized olivine-rich cumulates. They are predominantly composed of olivine, but also contain chlorite, serpentine, talc and magnetite. The iron-poor samples are from the

the ultramafic granulites or that the ultramafic rocks in the granulite belt were derived from slightly different magmas from those in the greenstone belts. On the Cr vs. MgO diagram (fig. 4) Cr increases with increasing MgO up to about 22% MgO; at higher MgO concentrations the trend flattens off and there is considerable scatter which may in part result from the redistribution of Cr during metamorphism. It is unlikely, however, that a difference of 3000 ppm Cr at 35% MgO can be explained entirely by this process, and it is probable that the scatter reflects the accumulation of Cr-poor olivine and Cr-rich pyroxene and chromite in some rocks and not in others.

layered dunite body at Hanga, where measured olivine compositions in chromite bearing rocks are Fo_{95}, although these are thought to have been enriched in Mg during metamorphism. It is unlikely that the observed difference in composition between the two types of serpentinite can be totally explained by the mobility of Fe and/or Mg during metamorphism since the process of serpentinization usually involves the loss of Fe (Condie, 1981) and yet the highly serpentinized samples are also the Fe-rich ones. Furthermore it is unlikely that alteration during metamorphism could double the Fe_2O_3 content of the serpentinite at these concentration levels. The Fe-rich and Fe-poor serpentinites are interpreted as olivine-rich cumulates of two different types. Olivine composition and magma-type are closely related (Roedder and Emslie, 1970) and the difference in cumulate type is taken to reflect two different magma-types in the Sierra Leone greenstone belts.

Roedder and Emslie (1970) showed that olivine composition in basic melts is a function of the MgO and FeO content of the liquid and the oxygen fugacity. Subsequent studies (Bender et al., 1978; Bickle et al., 1977) showed that the distribution coefficient $K_{D_{Fe-Mg}}^{oliv-liq}$ is also a function of temperature and pressure. The only rock types in this study which are known to represent liquid compositions are the basalts. They show a restricted range of MgO contents and a wide range of Fe_2O_3 contents. Assuming low-pressure fractionation, that all the iron is present in the reduced state, and adopting a $K_{D_{Fe-Mg}}^{oliv-liq} = 0.3$ (Bender et al., 1978; Roedder and Emslie, 1970) it is possible to derive the iron-rich olivine from basaltic compositions low in iron, and it is impossible to produce a Mg-rich olivine from these compositions. This, however, does not represent a unique solution for the origin of the iron-rich olivines and they may have been derived from a more iron-rich, picritic liquid, not represented by the analysed rock types.

Olivines with the composition Fo_{92-93} crystallized from a melt which was also precipitating chromite, indicating that the oxygen fugacity in the melt was low and that the iron was in the reduced state (Roedder and Emslie, 1970). These olivines must have evolved from a more magnesian liquid than that from which the iron-rich olivine was derived and it is likely therefore that the liquidus temperature was higher. In this case a lower value for the $K_{D_{Fe-Mg}}^{oliv-liq}$ is appropriate and a value of 0.24 was used (Bender et al., 1978). This necessitates that the liquid from which olivine Fo_{92-93} was derived had a MgO content $= 1.9$ $FeO_{(tot)}$. There is no certain way of estimating the FeO content of the liquid but MgO-rich liquids in other greenstone belts show a restricted range of iron contents

between 9.3 and 13.2% $FeO_{(tot)}$ (Nisbet et al., 1977; Nesbitt and Sun, 1976; Jahn et al., 1980). If this is also assumed for the Sierra Leone greenstone belts, olivines with the composition Fo_{92-93} were derived from a melt with an MgO content between 17.7 and 25.1%.

It is proposed therefore, that olivine-rich cumulates were derived from two different liquid compositions; iron-rich olivine cumulates, derived from basaltic or picritic liquids and iron-poor olivine cumulates derived from an ultramafic liquid with an MgO content of between 18 and 25 wt. %. The presence of an ultramafic liquid precipitating Fo_{92-93} and a basaltic or picritic liquid precipitating Fo_{85-86} does not preclude the two liquids from being related by fractional crystallization.

Basaltic rocks. Basaltic rocks with 5–10% MgO show a marked variation in Al_2O_3, $Fe_2O_{3(tot)}$, TiO_2, CaO, and Na_2O concentrations (fig. 3) although the high values of K_2O and Na_2O (Table II, fig. 3) indicate that most or all of the samples have been altered. However, a plot of major elements against TiO_2 for the Nimini belt basaltic rocks (fig. 5) shows some regular variations; there are strong positive correlations between $Fe_2O_{3(tot)}$ and TiO_2 and between P_2O_5 and TiO_2 ($TiO_2/P_2O_5 = 10$), and negative correlations between MgO and TiO_2 and Al_2O_3 and TiO_2, although the oxides SiO_2, CaO, Na_2O, and K_2O show a scatter which confirms element mobility, as discussed above.

There is also a good positive correlation between Ti and Zr for the Nimini amphibolites (fig. 6) which passes through the origin, indicating that there was no Ti in the fractionating phases in the upper
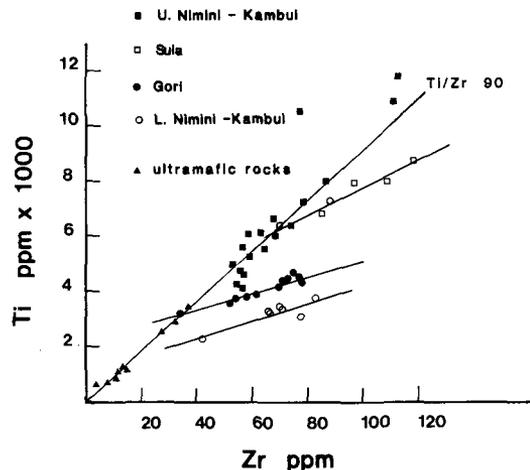

FIG. 6. Ti–Zr relations in amphibolites and ultramafic rocks from the Sierra Leone greenstone belts.

Table II Representative chemical analyses by X-ray fluorescence, of mafic and ultra mafic rocks from the greenstone belts of Sierra Leone

Rock	Amphibolites								Basic granulites		Ultramafic Rocks (Amphibolite facies)						Ultramafic Rocks (Granulite facies)			
	2^3	6^3	8^3	13^3	69	65	75	86	156	142	57	60	79	83	AJ1487	AJ103	159	160	178	170
SiO_2[1]	50.3	51.1	48.4	52.4	52.10	50.38	50.86	51.84	50.32	46.89	39.00	42.38	42.86	44.80	34.51	36.30	51.09	48.84	48.25	43.46
TiO_2	1.1	1.8	.8	.5	.40	1.33	.76	.62	.50	.87	.11	.19	.39	.56	nd	.06	.65	.48	.44	.27
Al_2O_3	12.4	11.9	12.9	14.0	15.12	15.91	12.58	15.17	13.90	15.27	2.33	4.99	8.42	9.84	1.22	.70	7.54	5.28	6.51	4.05
Fe_2O_3(tot)	13.4	14.9	12.1	10.4	9.30	12.60	12.70	11.73	11.65	13.50	12.18	10.64	12.58	13.33	13.19	6.77	11.91	11.43	13.18	12.51
MnO	0.2	0.2	0.2	0.2	.17	0.27	.31	.20	.21	.22	.20	.16	.21	.25	.18	.09	.20	.20	.23	.18
MgO	8.0	5.7	9.2	7.9	8.27	4.85	7.29	7.47	9.15	8.43	32.37	28.64	21.59	17.43	38.03	45.70	13.49	17.91	25.18	30.90
CaO	11.1	10.0	11.5	9.3	10.44	10.59	10.61	10.89	12.33	10.60	2.62	5.24	7.66	9.46	.44	1.20	14.07	13.51	5.72	5.19
Na_2O	2.0	2.5	2.3	3.0	2.42	3.63	2.67	2.52	2.24	3.02	.12	.27	.18	.74	.14	.03	1.84	1.54	.53	.91
K_2O	.2	.3	.1	1.3	.88	.14	.59	.17	.28	.51	.01	.03	.07	.08	.02	.02	.48	.39	.19	.93
P_2O_5	.1	.2	.1	.1	.11	.19	.14	.14	.14	.16	.05	.06	.10	.13	.02	.06	.16	.13	.11	.10
L.O.I.[4]	nd[6]	nd	nd	nd	1.00	.50	.33	1.00	.00	.42	10.67	7.58	5.83	3.66	11.90	7.28	.00	.45	.50	2.83
TOT	99.8	98.6	97.6	99.3	100.21	100.39	98.84	101.75	100.72	99.84	99.66	100.18	99.89	100.28	99.65	98.21	101.43	100.16	100.84	101.33
Cr[2,5]	259	154	375	459	274	322	811	383	261	269	4207	2982	4150	3107	5200	8143	1374	2464	3426	4217
Ni	121	73	178	125	75	123	151	66	132	155	1591	1491	997	818	nd	1870	274	518	963	1320
Zn	85	112	81	80	78	3	100	76	71	88	44	46	83	117	nd	nd	58	54	85	47
Rb	1	1	0	105	31	3	13	3	3	5	3	3	3	3	nd	nd	5	6	4	39
Sr	102	139	115	188	139	132	138	120	146	140	5	34	11	14	nd	nd	83	67	16	40
Y	24	31	21	18	10	26	15	17	13	21	3	4	10	13	nd	nd	13	9	9	10
Zr	74	111	56	78	42	87	77	51	34	47	7	12	26	36	nd	nd	46	29	29	21
Ba	34	49	30	300	231	36	159	49	40	10	3	3	3	3	nd	nd	38	3	3	6

1. All Major elements determined on fused discs using lithium tetraborate flux.

2. All trace elements determined on powders crushed to less than 90 mesh. Mass absorbtion corrections calculated from major element analysis from data published by Heinrich (1964).

3. All elements determined on pressed powder disc; rock ground to minus 240 mesh.

4. Uncorrected for Fe.

5. Uncorrected for the overlap of VKβ on CrKα. This is estimated to be 7ppm Cr for every 100ppm V present (Leake et al., 1969).

6. Not determined.

Localities and descriptions of analysed specimens:

2. Nimini, upper section; very fine grained hbl+plag+opq. Pseudomorphs after skeletal cpx.

6. Nimini, upper section; medium grained hbl+plag+opq. Polygonal plagioclase grains after original phenocrysts.

8. Nimini, upper section; medium grained hbl+plag+opq.

13. Nimini, lower section; medium grained hbl+plag; equigranular, weakly banded.

69. S. Kambui, lower section.

65. S. Kambui, upper section; medium grained hbl+plag+sphene+opq; equigranular, banded. Veins rich in plag, cc, sphene, epid.

75. Gori Hills; banded; coarse bands - hbl megacrysts+plag+sphene+epid+bi; fine bands - hbl+qz+plag.

86. Gori Hills; fine grained.

156. Bagla Hill (drill core); opx+cpx+opq+hbl+plag.

142. Lalehun; coarse grained cpx+opx+plag+hbl+opq.

57. S. Kambui; serpentinite cht+trem+serp+opq+olv.

60. S. Kambui; serpentinite.

79. Gori,part of layered sill; cht+trem+opq+cc; uralite pseudomorhs after opx.

83. Gori; as 79; banded fine and very fine trem +cht. Trem megacrysts overgrow uralite after opx.

AJ 1487 N. Kambui; serpentinite; coarse grained olv+trem+serp+cc+opq (anal. Andrew-Jones, 1968).

AJ 103 N. Kambui, Hanga; dunite (anal. Andrew-Jones, 1968).

159. Bagla Hill (drill core); equigranular opx+cpx+hbl(35%)+plag.

160. Bagla Hill (drill core); equigranular olv+opx+opq+hbl(40%)+bi.

178. Bagla Hill (drill core); equigranular olv+opx+hbl(45%)+bi+opq.

170. Bagla Hill (drill core); coarse, granular opx+hbl(40%)+opq+spinel(green).

(Hbl - hornblende; plag - plagioclase; opq - opaques; cc - calcite; epid - epidote; bi - biotite; qz - quartz; opx - orthopyroxene; cpx - clinopyroxene; cht - chlorite; trem - tremolite; olv - olivine; serp - serpentine)

Nimini basalts. In view of the incompatible nature of Ti in some basaltic liquids, its known absence from the fractionating phases in the upper Nimini basalts and its immobility during metamorphism, TiO_2 concentrations can be used to indicate igneous trends and as an index of the degree of partial melting or fractional crystallization (fig. 5).

The presence of plagioclase phenocrysts in the Nimini amphibolites indicates that a fractional crystallization model is a possible explanation for the observed major element trends in fig. 5. The depletion in Al_2O_3 and MgO and the enrichment in P_2O_5 and Fe_2O_3, with increasing TiO_2 implies the removal of an aluminous phase together with a magnesian phase or phases, or the removal of clinopyroxene. On the other hand, the trends in fig. 5 may relate to partial melting processes rather than fractional crystallization in which case TiO_2 and Fe_2O_3 decrease and MgO and Al_2O_3 increase in the melt with increasing degrees of partial melting. There is no evidence from the heavy REE concentrations from the upper Nimini basalts (fig. 8) that garnet was present in the source and so increasing Al_2O_3 in the melt would imply a plagioclase or spinel bearing source for these basalts.

The elements Ti, Zr, and Y are widely regarded as relatively immobile during metamorphism in basaltic rocks (Cann, 1969; 1970; Pearce and Cann, 1971; Smith and Smith, 1976; Humphries and Thompson, 1978; Vallance, 1974; Wood et al., 1976; Elliott, 1973). In view of the known mobility of some major elements during metamorphism greater weight is attached to petrogenetic arguments based on the immobile trace elements.

A plot of Ti vs. Zr for basaltic rocks in the upper and lower sections of the Nimini-Kambui belt, the Sula Mountains, and the Gori Hills defines different trends with different intercepts on the Ti axis (fig. 6). The Mano Moa granulites, however (not shown), scatter about the Nimini-Kambui upper section trend suggesting that Zr was mobile during granulite-facies metamorphism. The different Ti/Zr ratios for the upper and lower Nimini-Kambui, Sula, and Gori suites of basalts (fig. 6) indicate that they evolved in separate magma chambers and imply that they were erupted from geographically distinct volcanic centres.

In the upper Nimini-Kambui sequence Ti/Zr ratios are approximately constant and equal to 90 and are close to the suggested chondritic mantle ratio of 110 of Nesbitt and Sun (1976). The Ti/Zr ratio in the upper Nimini-Kambui sequence is identical to that found in ultramafic rocks intrusive into amphibolite in the Gori and Kambui belts (fig. 6). These data suggest that the basaltic liquids in the upper Nimini-Kambui succession and the ultramafic liquids in the Gori and Kambui belts were derived by the partial melting of a similar mantle

source, which was either depleted in Ti relative to a chondritic mantle or in which Ti was retained in either clinopyroxene or in an oxide phase during partial melting. This latter possibility is less likely in view of the much greater degree of melting necessary to produce the ultramafic rocks than the basaltic rocks.

Ti/Zr ratios in other belts are variable and range from 90-72 in the Sula Mountains, 90-60 in the Gori Hills, and 60-40 in the lower Nimini-Kambui sequence. The variation in Ti/Zr ratio suggests that either Ti was retained in the source during low degrees of partial melting or that there was fractionation of Ti-bearing phases at shallow crustal levels. The simplest explanation of the intercept of the Gori Hills and lower Nimini-Kambui curves with the Ti/Zr = 90 curve is that the Gori and lower Nimini-Kambui basalts were derived from a parental liquid with Ti/Zr = 90, followed by varying degrees of fractional crystallization of olivine ± a Ti-bearing phase or phases.

Zr/Y ratios are plotted on a logarithmic plot against Zr for basaltic compositions and some ultramafic rocks in fig. 7, and are shown relative to
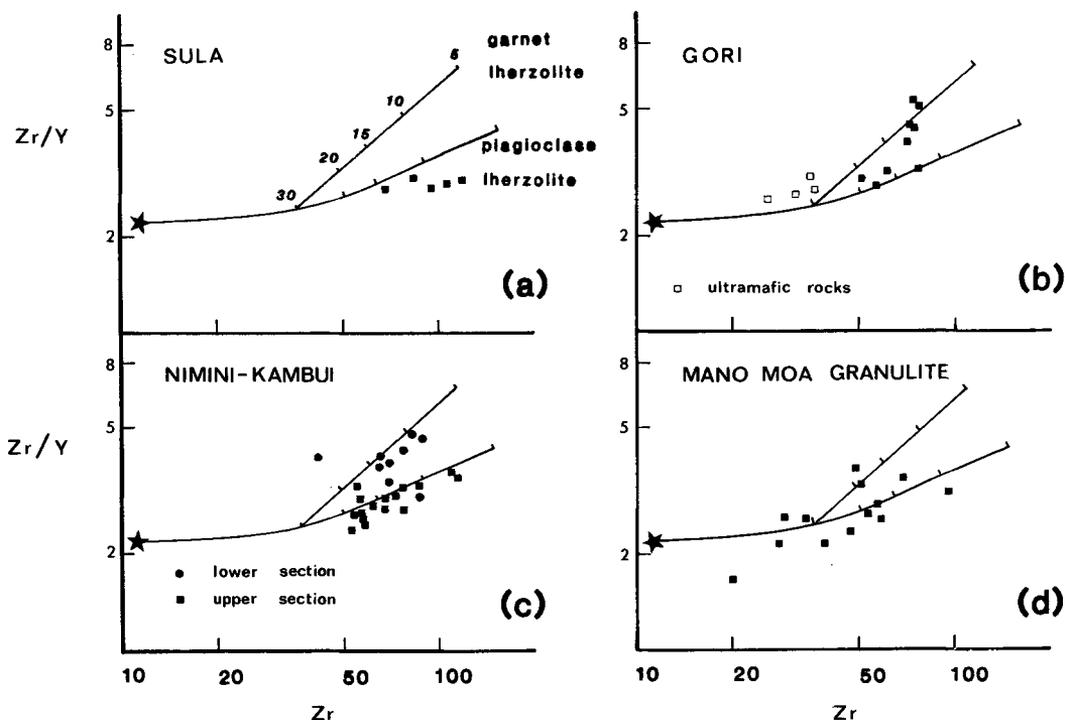

FIG. 7. Log–log plots of Zr/Y vs. Zr in the mafic and ultramafic rocks of the Sierra Leone greenstone belts. Reference curves are shown for the partial melting of a mantle source with 11 ppm Zr and 5 ppm Y (star) with the mineralogy of garnet lherzolite (upper curve) and plagioclase lherzolite (lower curve). The composition of the melt is shown for 5%, 10%, 15%, 20%, and 30% melting.

reference curves for the equilibrium melting of plagioclase lherzolite (lower curve) and garnet lherzolite (upper curve) source regions for a mantle containing 11 ppm Zr and 5 ppm Y (Sun and Nesbitt, 1977). The plagioclase lherzolite composition was assumed to be plag.$_{0.1}$, cpx$_{0.1}$, opx$_{0.2}$, oliv.$_{0.6}$ with the ratio of phases entering the melt as $4:4:1:3$. The garnet lherzolite composition was assumed to be garnet$_{0.1}$, cpx$_{0.1}$, opx$_{0.2}$, oliv. $_{0.6}$ and the ratio of phases entering the melt as $4:4:1:3$. Partition-coefficients for Zr and Y were calculated from the compilation of Pearce and Norry (1979).

Data points for each of the greenstone belt sequences plot in slightly different positions relative to the reference curves with the exception of the Mano Moa granulites which scatter about both curves and in which Zr is thought to have been mobile during metamorphism. The Zr/Y ratios vary in the Sula belt from 2.8 to 3.1, in the Gori belt from 2.8 to 5.2, in the Nimini–Kambui lower section from 2.4 to 3.6, and in the Nimini–Kambui upper section from 3.2 to 4.6. The only way in which the observed variation in Zr/Y can be achieved in the individual suites by fractional crystallization is by the fractionation of clinopyroxene. However, this would necessitate excessive amounts of crystal settling, for example up to 60% crystal fractionation is necessary to change the Zr/Y ratio in the upper Nimini-Kambui sequence from 2.4 to 3.6. Alternatively the range of Zr/Y ratios in the basalts may reflect the partial melting of a source region in which Y is retained to varying degrees in clinopyroxene and garnet. It is possible therefore that basalts from the Nimini–Kambui belt formed by 10–20% equilibrium partial melting of a garnet lherzolite source (lower section) and 8–20% partial melting of a plagioclase lherzolite source (upper section) (fig. 7c).

Rare earth element (REE) patterns were determined for five low-K tholeiites collected from the central part of the Nimini belt (upper section) where pillows and igneous textures are preserved and where chemical alteration is least pronounced. The analysed samples plot on the plagioclase lherzolite curve in fig. 7c and have Zr/Y ratios between 2.7 and 3.6.

Total REE concentrations are between 9 and 20 times chondrite values (Table III; fig. 8). Samples 2, 4, 8, and 11 show light REE enrichment, with (La/Sm)$_N$ between 1.1 and 1.5, flat to slightly depleted heavy REE with (Gd/Yb)$_N$ between 1.0 and 1.1 and with small negative Eu anomolies (fig. 8). Some samples show higher La concentrations than expected from the Ce and Nd values, and whilst there is no evidence that Ce has been altered by seawater, it is possible that there has been enrichment of La due to alteration during meta-

TABLE III. *Rare earth element concentrations (in ppm) in tholeiites from the Nimini belt*

	2	4	6	8	11
La	5.27	4.47	8.63	3.92	4.05
Ce	12.29	9.58	19.08	8.64	9.53
Nd	7.85	6.20	13.40	7.00	7.15
Sm	2.41	1.84	4.02	2.07	2.33
Eu	0.77	0.69	1.61	0.71	0.81
Gd	3.40	2.50	5.12	2.73	3.14
Dy	4.15	3.24	5.85	3.51	3.96
Er	2.50	2.11	3.40	2.31	2.59
Yb	2.43	1.97	nd	2.16	2.50

Determined by a mass spectrometric isotope dilution method as described by Hooker *et al.* (1975).

nd = not determined.

morphism. Similar variations in Eu concentrations may also be due to alteration during metamorphism (Sun and Nesbitt, 1978; Jahn and Sun, 1979). However, even allowing for the possible modification of the REE during metamorphism, sample 6 is different from the above samples in that it shows a greater degree of HREE depletion (Gd/Er)$_N$ = 1.23. The kick in the La concentration and the positive Eu anomoly are, however, possibly due to alteration during metamorphism.

Evidence from the range of Zr/Y ratios in the upper section Nimini basalts suggests that they could have been produced by 10–20% partial melting of a plagioclase lherzolite source with approximately 2.5 times chondrite concentrations of REE. This model was tested for the REE using the partition coefficients tabulated by Arth and Hanson (1975) and the non-modal melting parameters used above. It is possible to reproduce the observed REE patterns by the partial melting of a LREE depleted mantle source (Ce 1.8 times chondrite) with a flat HREE pattern (about 2.5 times chondrite HREE concentrations), followed by fractional crystallization. This would imply that the mantle source region for the upper Nimini basalts had undergone a previous melting episode. This is consistent with the stratigraphy inasmuch as these basalts are high in the stratigraphical succession and the basaltic rocks lower in the sequence may be the product of the earlier melting episode. A LREE depleted source is also consistent with the lower than chondritic Ti/Zr ratios in these rocks, although this feature is not confined to the Nimini belt.

Petrogenesis and discussion

One of the outstanding problems in the petrogenesis of greenstone belts is the relationship
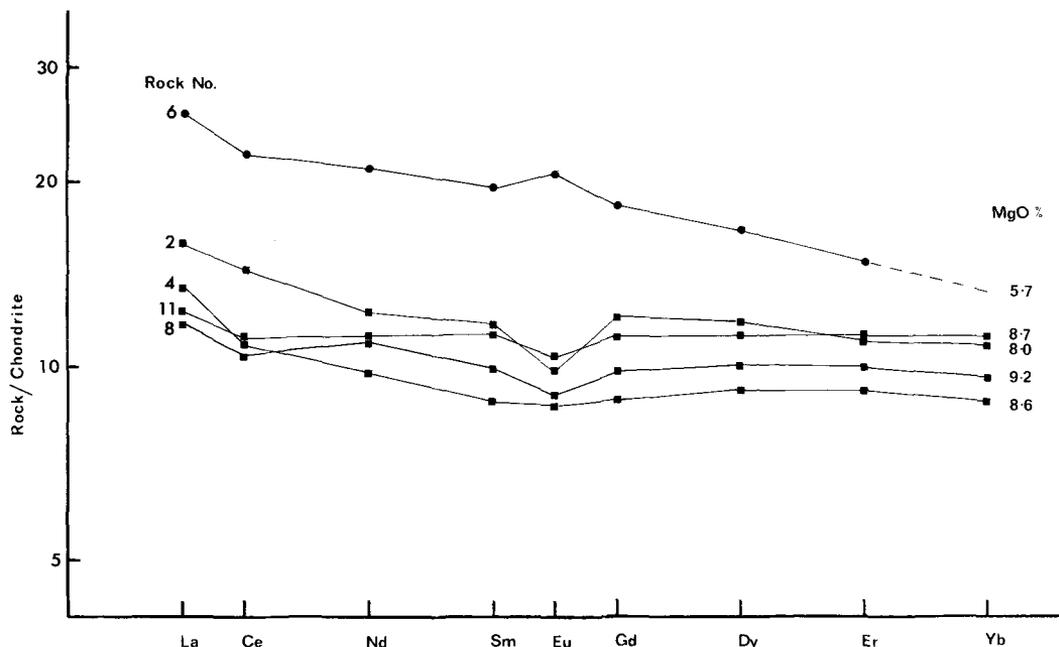
FIG. 8. *REE* patterns for amphibolites from the upper section of the Nimini belt. (Chondrite normalized after Nakamura, 1974.)

between the ultramafic rocks and the basalts. A number of models have been proposed.

(i) *The progressive melting of a rising mantle diapir.* In a rising mantle diapir initial melting at depth produces a basaltic liquid and the melt is erupted at the surface. As the diapir continues to rise melting ceases and the refractory harzburgite mantle rises on an adiabat until at shallow depth second-stage melting takes place to produce high-magnesian liquids. The advantage of this model is that it obviates the high degree of melting (40–60 %) necessary to produce an ultramafic liquid from the mantle (Arndt, 1977), an important problem in the genesis of ultramafic komatiites.

(ii) *Different degrees of partial melting of a similar mantle source.* Walker *et al.* (1980) and Stolper *et al.* (1981) have shown that the fraction of melt that can be stored in a mantle diapir is a function of the diapir size. They show that small (approx. 1 km) diapirs can build up a large fraction of melt (30 %), whereas large diapirs (10's of km) segregate small melt fractions. They propose that ultramafic komatiites represent the large melt fraction stored in a small diapir and that the tholeiites segregate from larger leaky diapirs, derived from a similar source region in the mantle.

(iii) *A basaltic magma chamber replenished by the periodic influx of an ultrabasic melt.* Huppert and Sparks (1980*a*, *b*) have shown that in a basaltic

magma chamber supplied by hot, dense ultrabasic liquid the two liquids are separated by a thermal boundary layer and that they remain compositionally distinct until the lower layer cools to the temperature of the upper layer and crystallizes olivine; at this point a residual basaltic liquid is released from the lower layer to mix with the upper basaltic layer. This model has been developed by Nisbet and Chinner (1981) to explain the intimate alternation of tholeiites and komatiites at Ruth Well, West Pilbara. They propose a transient magma chamber from which basalts, derived from parental komatiitic liquids, are erupted and that komatiites rise directly to the surface when the magma chamber is frozen.

In considering a model appropriate to the Sierra Leone greenstone belts the following lines of evidence must be taken into account: (*a*) *Sequence of intrusion.* In the greenstone belts of eastern Sierra Leone, the area discussed in detail in this paper, basaltic liquids were erupted *before* ultramafic liquids. However, in the Sula Mountains belt, in central Sierra Leone, ultramafic lavas were erupted before the basaltic lavas. Whilst it can be argued that in any one belt a full stratigraphic section may not be preserved, the pattern of magmatic evolution in the Sierra Leone greenstone belts is such that ultramafic rocks may be produced early or late in the history of individual belts. (*b*) There is field,

petrographic, and geochemical evidence for the existence of *two liquid compositions*. There is clear field evidence for the existence of basaltic liquids. Evidence from a plot of bulk compositions on an $Fe_2O_{3(tot)}$ *vs.* MgO diagram suggests that at least some of the olivine-rich cumulates were derived from liquids with between 18 and 25% MgO. (*c*) *Basalt trace element chemistry.* The observed variation in Zr/Y ratio in the basaltic rocks suggests that garnet was present in the source region of some of these rocks but not others and this implies that melting took place at different depths in the mantle. The *REE* evidence for the upper Nimini basalts suggests that they were derived from a mantle source region which had already suffered melt extraction. However, Ti/Zr ratios indicate that all basaltic rocks in the area are derived from a mantle source with a lower than chondritic Ti/Zr ratio.

Arth *et al.* (1977) used the progressive melting model to explain the intimate spatial relationship between tholeiites and komatiites in Munro Township, Ontario. The model also works well for the greenstone belts of eastern Sierra Leone, where it has been shown that the ultramafic rocks post-date the basalts. It is not consistent, however, with the stratigraphical relationships in the Sula Mountains belt in central Sierra Leone, where ultramafic lavas are the first liquids to be produced and these are followed by basalts. The model of Walker *et al.* (1980) and Stolper *et al.* (1981) based upon diapir size, however, is consistent with the observed field relationships except for the base of the succession in the Nimini belt where basaltic rocks and ultramafic flows alternate (fig. 2). The implications of this model are that in central Sierra Leone an early, small diapir supplying ultramafic liquids was followed by a larger diapir supplying basaltic liquids. In the east of Sierra Leone, however, a large early diapir supplied basaltic liquids to the surface as it rose to successively shallower depths and was followed by a smaller diapir supplying ultramafic liquids.

Of the three models, however, the replenished magma chamber model is the most versatile in explaining the field relationships between the ultramafic and basaltic rocks. It is also consistent with the Ti/Zr ratios which suggest a genetic relationship between the ultramafic and basaltic liquids. On the other hand the model does not easily explain the observed Zr/Y ratios; the high degrees of melting necessary to produce the parental high magnesian liquids would eliminate most of the clinopyroxene and garnet from the source so that Y could not be retained in the source during melting. Subsequent fractional crystallization of olivine and spinel would not produce the observed variation in Zr/Y, although it may be possible to explain it in terms of clinopyroxene fractionation. Alternatively the Zr/Y ratios reflect chemical heterogeneity in the source region; this means that in the Gori Hills belt, for example, successive basaltic melts were derived from regions in the mantle with different Zr/Y ratios.

It is not possible on the basis of the available data to choose between the last two models.

REFERENCES

Allegre, C. J., Treuil, M., Minster, J. F., Minster, B., and Albarede, F. (1977) *Contrib. Mineral. Petrol.* **60**, 57–75.
Andrews-Jones, D. A. (1968) Ph.D. thesis, Univ. Leeds.
Arndt, N. T. (1977) *Contrib. Mineral. Petrol.* **64**, 205–21.
Arth, J. G., and Hanson, G. N. (1975) *Geochim. Cosmochim. Acta*, **39**, 325–62.
——Arndt, N. T., and Naldrett, A. J. (1977) *Geology*, **5**, 590–4.
Beckinsale, R. D., Gale, N. H., Macfarlane, A., Crow, M. J., Arthurs, J. W., and Wilkinson, A. F. (1980) *Precambrian Res.* **13**, 63–76.
Bender, J. F., Hodges, F. N., and Bence, A. E. (1978) *Earth Planet. Sci. Lett.* **41**, 277–302.
Bickle, M. J., Ford, C. E., and Nisbet, E. G. (1977) *Ibid.* **37**, 97–106.
Cann, J. R. (1969) *J. Petrol.* **10**, 1–19.
——(1970) *Earth Planet. Sci. Lett.* **10**, 7–11.
Condie, K. C. (1981) *Archaean Greenstone Belts.* Elsevier.
Dunham, K. C., Phillips, R., Chalmers, R. A., and Jones, D. A. (1958) *Bull. Overseas Geol. Mineral. Res. Suppl.* **3**, 44 pp.
Elliott, R. B. (1973) *Contrib. Mineral. Petrol.* **38**, 71–9.
Hart, S. R., and Davis, K. E. (1978) *Earth Planet. Sci. Lett.* **40**, 203–19.
Heinrich, K. F. J. (1964) In *The Electron Microscope* (McKinley, T. D., Heinrich, K. F. J., and Wittry, D. B., Eds.). New York: Wiley, 296–377.
Hooker, P. J., O'Nions, R. K., and Pankhurst, R. J. (1975) *Chem. Geol.* **16**, 181–96.
Humphries, S. E., and Thompson, G. (1978) *Geochim. Cosmochim. Acta*, **42**, 127–36.
Huppert, H. E., and Sparks, R. S. J. (1980*a*) *Nature*, **286**, 46–8.
————(1980*b*) *Contrib. Mineral. Petrol.* **75**, 279–89.
Jahn, B. M., and Sun, S. S. (1979) *Phys. Chem. Earth*, **11**, 597–618.
——Auvray, B., Blais, S., Capdevila, R., Cornichet, J., Vidal, F., and Hameurt, J. (1980) *J. Petrol.* **21**, 201–44.
Leake, B. E., Hendry, G. L., Kemp, A., Plant, A. G., Harrey, P. K., Wilson, J. R., Coats, J. S., Aucott, J. W.,

Lunel, T., and Howarth, R. J. (1969) *Chem. Geol.* **5**, 7–86.

MacFarlane, A., Crow, M. J., Arthurs, J. W., and Wilkinson, A. F. (1981) *Overseas Mem. Inst. Geol. Sci.* **7**, 103 pp.

Marmo, V. (1962) *Bull. Geol. Surv. Sierra Leone.* **2**, 117 pp.

Muecke, G. K., Pride, C., and Sarkar, P. (1979) In *Origin and Distribution of the Elements*, **2** (L. H. Ahrens, ed.). Pergamon, London.

Nakamura, N. (1974) *Geochim. Cosmochim. Acta*, **38**, 757–75.

Nesbitt, R. W., and Sun, S. S. (1976) *Earth Planet. Sci. Lett.* **31**, 433–53.

Nisbet, E. G., Bickle, N. J., and Martin, A. (1977) *J. Petrol.* **18**, 521–66.

—— and Chinner, G. A. (1981) *Econ. Geol.* **76**, 1729–35.

Pearce, J. A. (1978) Abstract in Rea, W. J. (ed.). *J. Geol. Soc. Lond.* **135**, 591.

—— and Cann, J. R. (1971) *Earth Planet. Sci. Lett.* **12**, 339–49.

—— and Norry, M. J. (1979) *Contrib. Mineral. Petrol.* **69**, 33–47.

Roedder, P. L., and Emslie, R. F. (1970) Ibid. **29**, 275–82.

—— Campbell, I. H., and Jamieson, H. E. (1979) Ibid. **68**, 325–34.

Rollinson, H. R. (1978) *Nature*, **272**, 440–2.

—— (1982) *Earth Planet. Sci. Lett.* **59**, 177–91.

—— and Cliff, R. A. (1982) *Precambrian Res.* **17**, 63–72.

Schreyer, W., Werding, G., and Abraham, K. (1981) *J. Petrol.* **22**, 191–231.

Simkin, T., and Smith, J. V. (1970) *J. Geol.* **78**, 304–25.

Smith, R. E., and Smith, S. E. (1976) *Earth Planet. Sci. Lett.* **32**, 114–20.

Stolper, E., Walker, D., Hager, B. H., and Hays, J. F. (1981) *J. Geophys. Res.* **86**, 6261–71.

Sun, S. S., and Nesbitt, R. W. (1977) *Earth Planet. Sci. Lett.* **35**, 429–48.

—— —— (1978) *Contrib. Mineral. Petrol.* **65**, 301–25.

Vallance, T. G. (1974) *J. Petrol.* **15**, 79–96.

Walker, D., Stolper, E. M., and Hays, J. P. (1980) *EOS* **61**, 385 (abs.).

Williams, H. R. (1978) *Precambrian Res.* **6**, 251–68.

Wilson, N. W., and Marmo, V. (1958) *Bull. Geol. Surv. Sierra Leone*, **1**, 91 pp.

Wood, D. A., Gibson, I. L., and Thompson, R. N. (1976) *Contrib. Mineral. Petrol.* **55**, 241–54.